

## Palaeomagnetism of Middle Ordovician Carbonate Sequence, Vaivara Sinimäed Area, Northeast Estonia, Baltica

Jüri PLADO<sup>1</sup>, Ulla PREDEN<sup>1,2</sup>, Argo JÕELEHT<sup>1</sup>, Lauri J. PESONEN<sup>3</sup>,  
and Satu MERTANEN<sup>4</sup>

<sup>1</sup>Department of Geology, University of Tartu, Tartu, Estonia;  
e-mail: juri.plado@ut.ee

<sup>2</sup>Põlva County Government, Põlva, Estonia

<sup>3</sup>Division of Physics, University of Helsinki, Helsinki, Finland

<sup>4</sup>Geological Survey of Finland, Espoo, Finland

### Abstract

The hill range of Vaivara Sinimäed in northeast Estonia consists of several narrow east- to northeast-trending glaciotectonic fold structures. The folds include tilted (dips 4-75°) Middle Ordovician (early Darriwilian) layered carbonate strata that were studied by mineralogical, palaeomagnetic, and rock magnetic methods in order to specify the post-sedimentational history of the area and to obtain a better control over the palaeogeographic position of Baltica during the Ordovician. Mineralogical studies revealed that (titano)magnetite, hematite, and goethite are carriers of magnetization. Based on data from 5 sites that positively passed a DC tilt test, a south-easterly downward directed component A ( $D_{\text{ref}} = 154.6^\circ \pm 15.3^\circ$ ,  $I_{\text{ref}} = 60.9^\circ \pm 9.7^\circ$ ) was identified. The component is carried by (titano)magnetite, dates to the Middle Ordovician ( $Plat = 17.9^\circ$ ,  $Plon = 47.3^\circ$ ,  $K = 46.7$ ,  $A95 = 11.3^\circ$ ), and places Baltica at mid-southerly latitudes. Observations suggest that in sites that do not

pass the tilt test, the glaciotectonic event has caused some rotation of blocks around their vertical axis.

**Key words:** Baltica plate, Estonia, Ordovician, rock magnetism, palaeomagnetism.

## 1. GEOLOGICAL SETTING

The study area is located in western part of the East European Platform (part of Baltica plate) and is regionally characterized by relatively flat topography and homoclinal bedding of sedimentary strata. Here, the southern slope of the Precambrian Fennoscandian Shield is covered by Ediacaran to Middle Ordovician sedimentary rocks that are dipping southerly at low angle (8-11'; Vaher *et al.* 2013). An outstanding topographic feature in the area is the 20-35 m high Baltic Clint (Fig. 1) where Cambrian and Ordovician sediments crop out. The area also includes folds, diapir-like features of the Lower Cambrian clay, and uplifted blocks of Cambrian siliciclastic and Ordovician carbonate rocks (Fig. 1D). Genesis and timing of these structures have been linked to two possibly coeval processes: (i) lateral movements by the Scandinavian Ice Sheet and (ii) vertical movements due to diapiric processes (*e.g.*, Jaansoon-Orviku 1926, Rattas and Kalm 2004, Vaher *et al.* 2013). The most prominent of these structures are located between Laagna and Puhkova villages (Fig. 1) being up to 1.5 km long and 15-20 m high. Similar structures that are composed of Middle Ordovician carbonates in their upper outcropping part, the Vaivara Sinimäed in Tornimägi and Pargimägi areas (Fig. 1), are interpreted as Quaternary ice marginal formations (Miidel *et al.* 1969). The orientation of fold axes is generally to the east or northeast and they do not have roots in the crystalline basement (Puura and Vaher 1997) that is located ~200 m deep as based on drillings. Most of the vertical movements are related to thinning or thickening of the Lower Cambrian clays that occasionally attain double thickness. The exact mechanism of clay thickening and extent of lateral movement of overlaying strata is not clear. The morphology of topographic features suggests that some blocks have been transported to some extent whereas some blocks show no obvious lateral movement. Supposedly, blocks with larger lateral movement have also been rotated around their vertical axes as stress in glacio-marginal conditions is not necessarily uni-directional. Our option is to determine nature of folding and possible rotations applying palaeomagnetic, rock magnetic, and mineralogical methods on these rocks. In addition, we attempt to obtain a better control over the palaeogeographic position of the Baltic Plate for the early Darriwilian Stage (Middle Ordovician).

The strata above Lower Cambrian clays involve the Cambrian and Ordovician siliciclastic rocks (no stable remanence components obtained) and

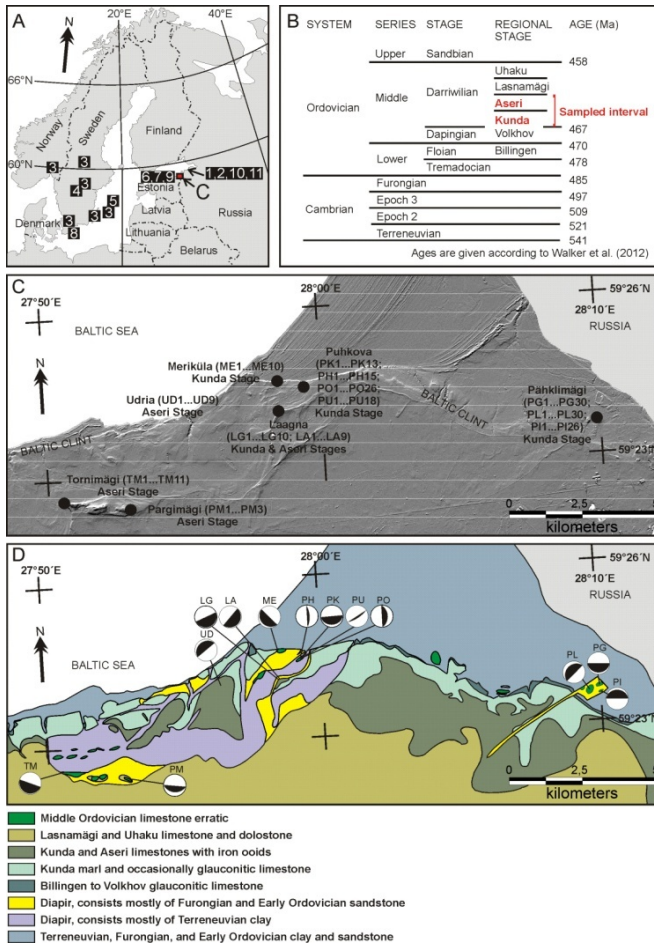


Fig. 1: (A) Location of the study area in northern Europe. Numbers refer to locations of earlier studies of Lower and Middle Ordovician sequences by various authors (1, 10, and 12 by Khramov and Iosifidi (2009); 2 and 11 by Smethurst *et al.* (1998); 3 by Perroud *et al.* (1992), 4 by Torsvik *et al.* (1995), 5 by Claesson (1978); 6, 7, and 9 by Plado *et al.* (2010); 8 by Torsvik and Rehnström (2003)) and are represented in accordance with information in Fig. 6B. (B) Stratigraphic scheme for the Middle Ordovician in Estonia indicating position of sampled regional stages (Aseri and Kunda). (C) Sampling locations in NE Estonia. Coordinates and structural information are given in Table 1. The base map represents shadowed topography (based on data from Estonian Land Board) where the E-W-oriented Baltic Clint separates the Ordovician plateau in south from the northern lowland. The plateau has thin layer of Quaternary sediments whereas in the lowland the Cambrian sediments are covered with sediments of glacial, marine and/or organic origin. (D) A simplified geological map of the area after Suuroja *et al.* (2009). Stereoplots illustrate structural elements of limestone layers in sampled locations (Table 1).

Table 1

Sampling site locations, their coordinates,  
and structural information used for tilt correction

| Location   | Site | <i>N/n</i> | Coordinates<br>(WGS84) |         | Dip<br>azimuth<br>[°] | Dip<br>[°] |
|------------|------|------------|------------------------|---------|-----------------------|------------|
|            |      |            | N [°]                  | E [°]   |                       |            |
| Tornimägi  | TM   | 9/12       | 59.3772                | 27.8425 | 203                   | 4          |
| Pargimägi  | PM   | 3/38       | 59.3736                | 27.8819 | 188                   | 30         |
| Udria      | UD   | 9/ 9       | 59.4009                | 27.9392 | 323                   | 14         |
| Laagna     | LG   | 10/19      | 59.4018                | 27.9688 | 158                   | 4          |
|            | LA   | 9/15       | 59.4010                | 27.9728 | 133                   | 5          |
| Meriküla   | ME   | 10/13      | 59.4109                | 27.9742 | 228                   | 11         |
| Puhkova    | PH   | 14/14      | 59.4086                | 27.9913 | 303                   | 63         |
|            | PK   | 12/19      | 59.4092                | 27.9910 | 178                   | 15         |
|            | PU   | 18/21      | 59.4080                | 27.9879 | 145-153               | 65-75      |
|            | PO   | 26/29      | 59.4080                | 27.9903 | 303                   | 35         |
| Pähklimägi | PG   | 30/36      | 59.3945                | 28.1671 | 183                   | 10         |
|            | PL   | 31/31      | 59.3932                | 28.1614 | 318                   | 13         |
|            | PI   | 26/36      | 59.3927                | 28.1670 | 3                     | 12         |

**Notice:** Sites are shown in Fig. 1. *N* = number of cores (hand samples in Pargimägi); *n* = number of specimens.

Ordovician carbonate rocks. The latter are known (Khramov and Iosifidi 2009, Plado *et al.* 2010) to carry primary remanence. Based on geological mapping results (Suuroja *et al.* 2009), the total thickness of Middle Ordovician sequence in NE Estonia is 35 to 40 m, being represented by five regional stages (see Fig. 1B and D). The sampled carbonate rocks belong to the Kunda and Aseri regional stages, which represent the older part of the Darriwilian Stage (467-458 Ma see Walker *et al.* (2012), Fig. 1B) and are composed of argillaceous, occasionally bioclastic and partly dolomitized limestones. Thicknesses of formations corresponding to the Kunda and Aseri Stages are of about 8 and 3 m, respectively. The uppermost 2 m of the Kunda and the whole Aseri limestones contain ferriferous (goethitic) ooids. Occasionally, the Kunda limestones contain mm-sized glauconite grains.

Our earlier palaeomagnetic studies (Plado *et al.* 2010), which included the region under discussion, concentrated mostly on reddish and fully dolomitized varieties of carbonate rocks that occur close to regional fracture zones without upheaval movements. Mineralogical and palaeomagnetic studies revealed that hematite causes the reddish colour of the rocks, is of secondary origin and dates to the Middle to Late Permian ages. In the present

study, which concentrates to local glaciotectonic features, the reddish varieties were met rarely.

## 2. SAMPLES AND METHODS

Two hundred seven oriented mini-drill cores and three hand samples (Pargimägi site) were collected from 13 sites representing Kunda to Aseri stage carbonate rocks in 7 locations (Fig. 1) in 2009 and 2010. The sites (outcrops) consisted of strata that are tilted at various angles ranging from 4 to 75° (Table 1; Fig. 1). Two hundred ninety two standard cylindrical specimens were prepared. The rock- and palaeomagnetic studies were carried out in the Laboratory for Solid Earth Geophysics of the University of Helsinki and in the Geophysics Laboratory of the Geological Survey of Finland.

Mineralogy of 13 samples was studied in thin sections by polarization microscope (Leica DM2500P; 10 thin sections) and powdered whole rock samples with X-ray diffractometry (Dron-3M diffractometer; 3 samples) at the Department of Geology, University of Tartu. Scanning electron microscopy (SEM; JEOL JSM-5900LV) studies with X-ray microanalysis (Energy Dispersive X-ray Spectroscopy) were performed at the laboratory of the Geological Survey of Finland (3 thin sections).

The magnetic measurements consisted of production of IRM (Isothermal Remanent Magnetization) acquisition curves for 12 specimens using a Molspin pulse magnetizer with the maximum field of 1.5 T and thermal demagnetization of triaxial IRM-acquisition components (Lowrie 1990, 17 steps up to 680°C) for 10 specimens. The Lowrie tests were performed after IRM acquisition at 1.5, 0.4, and 0.12 T fields along the *z*, *y*, and *x* axis, respectively. Temperature dependence of magnetic susceptibility of eight powdered whole rock samples was performed with AGICO's KLY-3S Kappabridge by heating the powdered specimens in an inert (Ar) gas atmosphere from room temperature up to 700°C and back to 40°C. The low temperature (-193 to 0°C) thermomagnetic measurements were conducted for three samples. Hysteresis (using Princeton Measurement Corporation MicroMag<sup>TM</sup>3900 Vibrating Sample Magnetometer with maximum available field of 1 T) of eight samples was measured.

For palaeomagnetic studies, the specimens were stepwise demagnetized with alternating field (AF) up to 160 mT and/or thermally (TH); up to 680°C). In a case of specimens with abundant goethite ooids carrying a viscous or unstable component, specimens were first thermally demagnetized up to 120°C, followed by AF and, if needed, again by TH. In several cases, the demagnetization was terminated earlier, if the intensity of NRM decreased below the level of instrumental noise ( $\sim 0.03 \text{ mAm}^{-1}$ ) or increased significantly due to mineralogical changes during the TH treatment. After

each step, intensity and direction of NRM were measured using a superconducting (2G Model 755 DC SQUID) magnetometer. Individual NRM measurements were subjected to a joint analysis of stereographic plots, intensity decay curves, orthogonal vector diagrams (Zijderveld 1967) and principal component analysis (Kirschvink 1980) to obtain the characteristic remanence (ChRM) directions. Fisher (1953) statistics was used to calculate mean remanence directions. GMAP software (Torsvik and Smethurst 1999) was used for palaeogeographic reconstruction.

### 3. RESULTS

#### 3.1 Mineralogy

The studied carbonate rocks are rich in shelly fossils (krinoids, ostracodes, bryozoans, and fragments of brachiopods, molluscs, and trilobites)

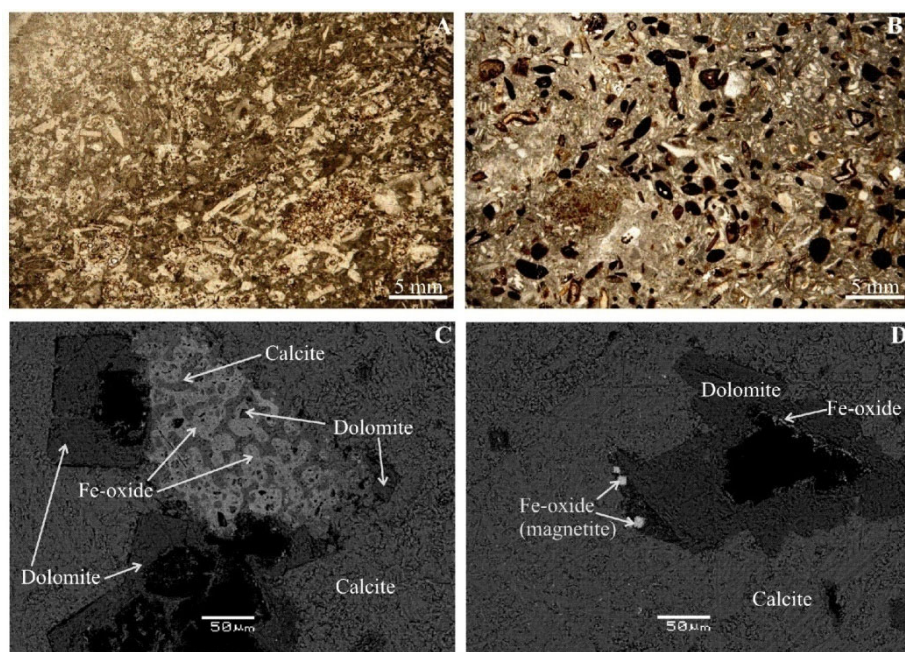


Fig. 2. Optical microscope (A & B) and backscattered scanning electron microscope (C & D) images of carbonates. (A) Fossil detrite-rich and partly dolomitized carbonate from Pargimägi (plane polarized light; sample PM1). (B) Large goethite ooids (dark grains) from Udria carbonates (plane polarized light; sample UD3). (C) Fossil exoskeletons filled with iron oxide and euhedral dolomite crystals in calcite matrix (sample LA2 from Laagna). (D) Large (5-10 μm) magnetite crystals and iron oxide mass are related to the formation of dolomite (sample PM3 from Pargimägi).

and are partly dolomitized (Fig. 2A). On the basis of XRD analyses, the studied carbonates mainly consist of dia- and paramagnetic minerals as calcite (30-80 %), dolomite (7-60 %), clay minerals (1-7 %; mainly illite), K-feldspar (3-4 %), quartz (1-2 %), and apatite (1 %). Ferromagnetic minerals were not detected with XRD due to low concentration (<1 %). Iron-rich minerals were, however, observed in thin sections as goethite ooids in Udria (Fig. 2B) and Tornimägi sections. Udria and Tornimägi varieties have, compared to rocks from other sites, relatively high whole-rock magnetic susceptibilities. Reddish patches that represent aggregates of hematite concentrated in or near the dolomite crystals or filling the voids of fossil exoskeletons (Fig. 2C), and grains of magnetite (identified by SEM X-ray microanalysis, Fig. 2D) were identified. In addition, titanium-iron oxides and grains of pyrite were detected.

### 3.2 Rock magnetism

Coercivity parameters determined by IRM and hysteresis data, demagnetization behaviour (Lowrie tests), and thermomagnetic analyses all indicate that the magnetic mineral assemblage is dominated by a complex mixture of ferromagnetic minerals that includes (Ti-)magnetite, hematite, and goethite.

For most samples, IRM-acquisition curves are far from saturation at the maximum field (1.5 T, Fig. 3A), indicating the presence of a highly coercive ferromagnetic mineral or a mixture of high- to low-coercive minerals. Presence of low-coercivity (<100 mT) fraction is observed in Pargimägi (samples PM1 and PM3), Tornimägi (TM6 and TM10), and Laagna (LA7) sites. Results of the Lowrie (1990) tests, *i.e.* stepwise TH demagnetization of a three-axis IRM, are shown in Figs. 3B-E. Most of the analyses showed results similar to that given by Fig. 3B, where the IRM in soft and medium coercivity fraction was removed at 520-560°C, referring to unblocking temperature of magnetite. Hard coercivity minerals are, however, also present. First, there is major decrease of intensity in hard coercivity component at 120°C (Figs. 3B and E) typical for goethite (*e.g.*, Özdemir and Dunlop 1996). Second, a drop of intensity is observed at 640-680°C and is caused by hematite (Figs. 3D). As the TH demagnetization during the palaeomagnetic studies (see below) fails to identify hematite-carried component, the second signal may partly be due to thermally (lab-) produced hematite.

During the thermomagnetic study (Figs. 4A and B), every single measurement showed irreversible cooling curve indicating growth on new minerals during the heating despite an inert atmosphere used in the furnace. Low values of magnetic susceptibility and the linear or slightly hyperbolic shape of the initial curve correspond to a dominant dia- and/or paramagnetic

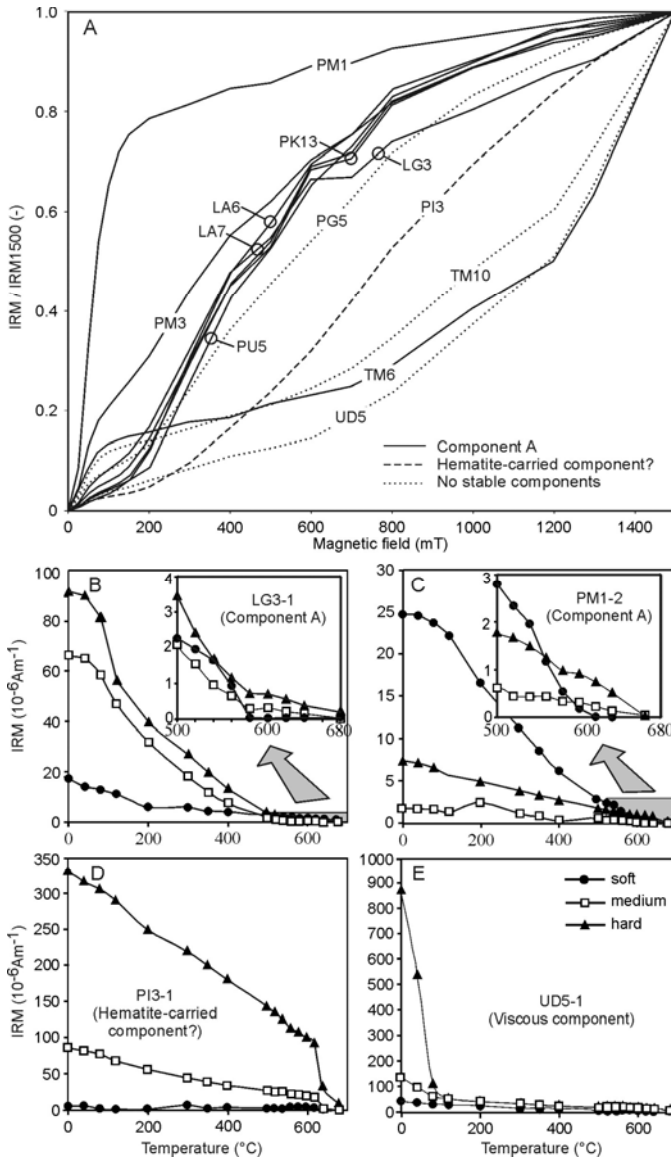


Fig. 3: (A) Progressive acquisition of IRM. Style of curves indicates appearance or lack of palaeomagnetic components in corresponding specimens. (B-E) The Lowrie (1990) test curves, *i.e.* thermal demagnetization curves of IRM<sub>z</sub>'s produced by magnetizing the sample in 1.5 T along the z-axis, followed by 0.4 T along the y-axis and 0.12 T along the x-axis for studied carbonates. The soft, medium, and hard components are shown during thermal demagnetization. For sample locations see Fig. 1. The occurrence of remanence component in certain specimen is indicated. Inserts in B and C enlarge information at the high-temperature ends.



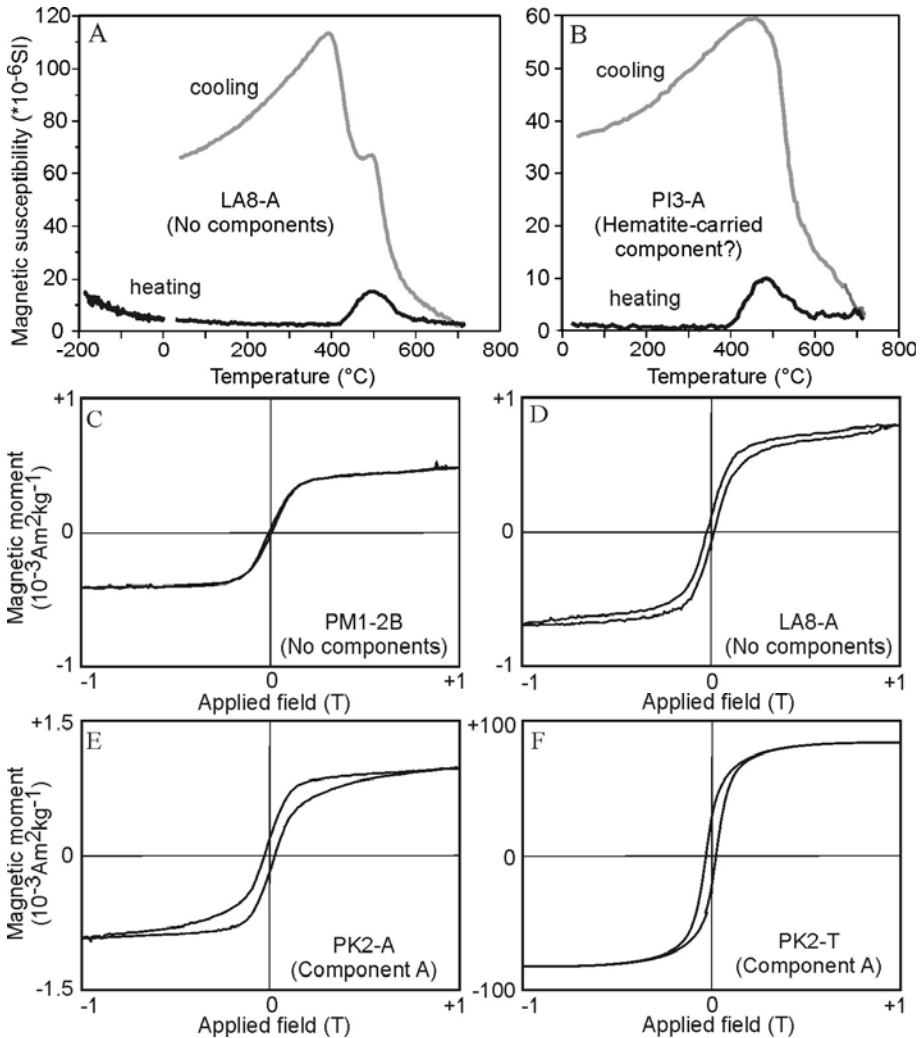


Fig. 4. Examples of magnetic susceptibility versus temperature measurements of sample from (A) Laagna and Pähklmägi (B) locations. The measurements were carried out in an argon atmosphere. Appearance of palaeomagnetic components is indicated. (C-F) Hysteresis loops after correction for paramagnetic contribution for three representative natural samples from (C) Pargimägi, (D) Laagna, (E) Puhkova, and (F) heated (after thermomagnetic analysis) Puhkova sample.

behaviour. An increase of the magnetic susceptibility is observed at 400–500°C, falling after 580°C, indicating the presence of newly formed magnetite. There are several candidates for new-formed magnetite: breakdown of smectite at 200–500°C (Hirt *et al.* 1993), alteration of pyrite (Tarling 1983),

or reduction of hematite into magnetite (*e.g.*, Shive and Diehl 1997). Due to these major mineralogical changes, the results that were acquired during thermal demagnetization at temperatures  $> 400^{\circ}\text{C}$  were not applicable for palaeomagnetic interpretation. An attempt to record the low-temperature (from about  $-195^{\circ}\text{C}$  to room temperature; Fig. 4A) susceptibility gave no meaningful results

Hysteresis properties (Fig. 4) include correction against the paramagnetic effect. The correction has also obliterated signals by goethite/hematite, but not fully, as some of the curves show no full saturation. Majority of hysteresis loops are slightly wasp-waisted indicative for coexisting at least two magnetic components with contrasting coercivities (Roberts *et al.* 1995). The experiments where the hysteresis of the same specimen was measured before and after the heating cycle (Figs. 4E and F) showed that heating increased the ferromagnetic signal, which affirms production of new ferromagnetic minerals during heating.

### 3.3 Palaeomagnetic behaviour

A characteristic remanent magnetization (ChRM) component (hereafter called component A) was identified (Table 2; Fig. 5) at 9 (out of 13) sites. The component A is of intermediate coercivity (removed at fields up to 60 mT). During the course of thermal demagnetization, A is observable up to  $300\text{--}400^{\circ}\text{C}$ , after which an abrupt increase in magnetic susceptibility and/or intensity of the NRM occurs, indicating mineralogical changes obscuring the observations. Comparing the demagnetization results with the thermomagnetic, hysteresis, and IRM studies, we suggest that the principal carrier of component A is single to pseudo-single domain (Ti-) magnetite.

Other components that are more resistant to AF demagnetization, and not removed during the AF treatment at 160 mT, exist within the studied lithologies. One of them, unblocking at temperature of  $120^{\circ}\text{C}$ , correlates with samples including goethitic iron ooids. The component carried by goethite tends to be directed NE, a direction close to the Present Earth Field (PEF:  $D \approx 9^{\circ}$ ;  $I \approx 73^{\circ}$ ). Another highly coercive component, likely carried by hematite, is present in two Pähklimägi sites (PI and PG) only. Because of mineralogical changes taking part during the thermal treatment, we were unable to separate this component with confidence.

The locally dolomitized limestones from Tornimägi (TM) with biomorphic texture are mildly ( $4^{\circ}$ ) tilted southwards. The limestones contain goethitic iron ooids and hematite; the latter is related to the voids of fossil exoskeletons. Based on IRM studies, the rocks include both intermediate and high coercively phases, but only the intermediate coercivity component (A)

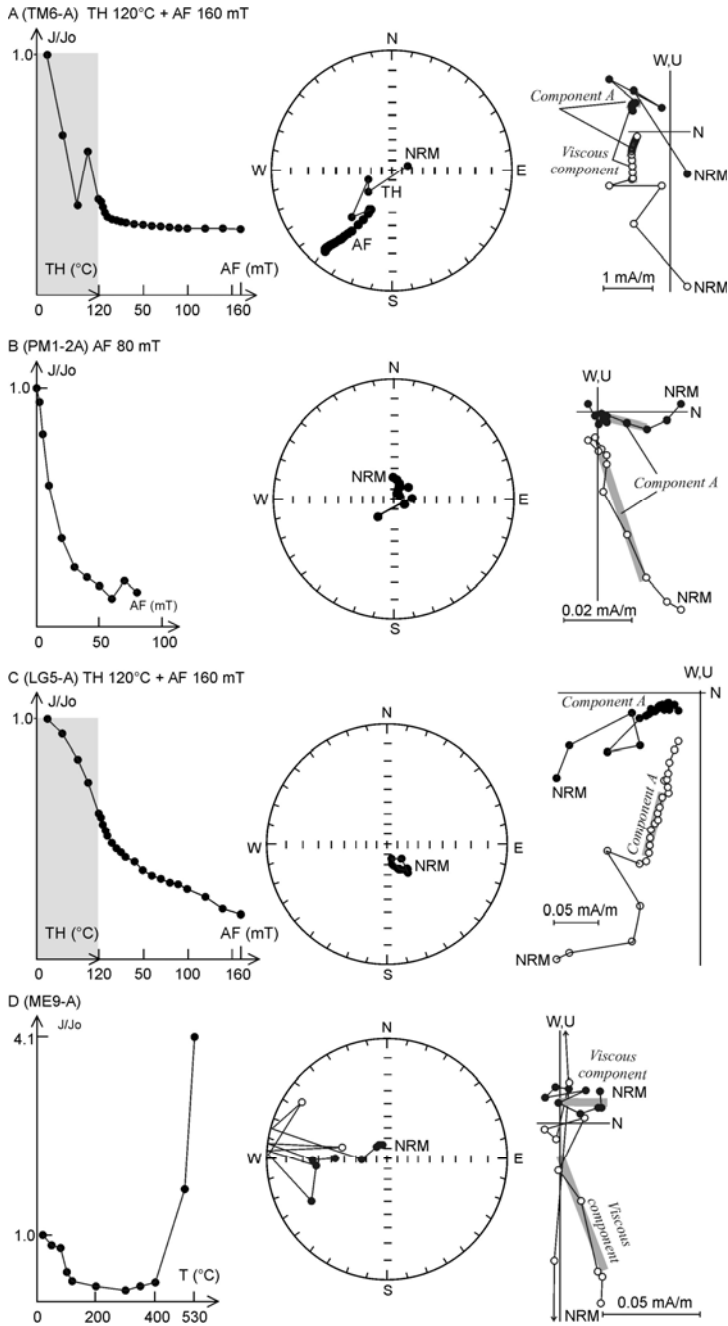


Fig 5. Continued on next page.

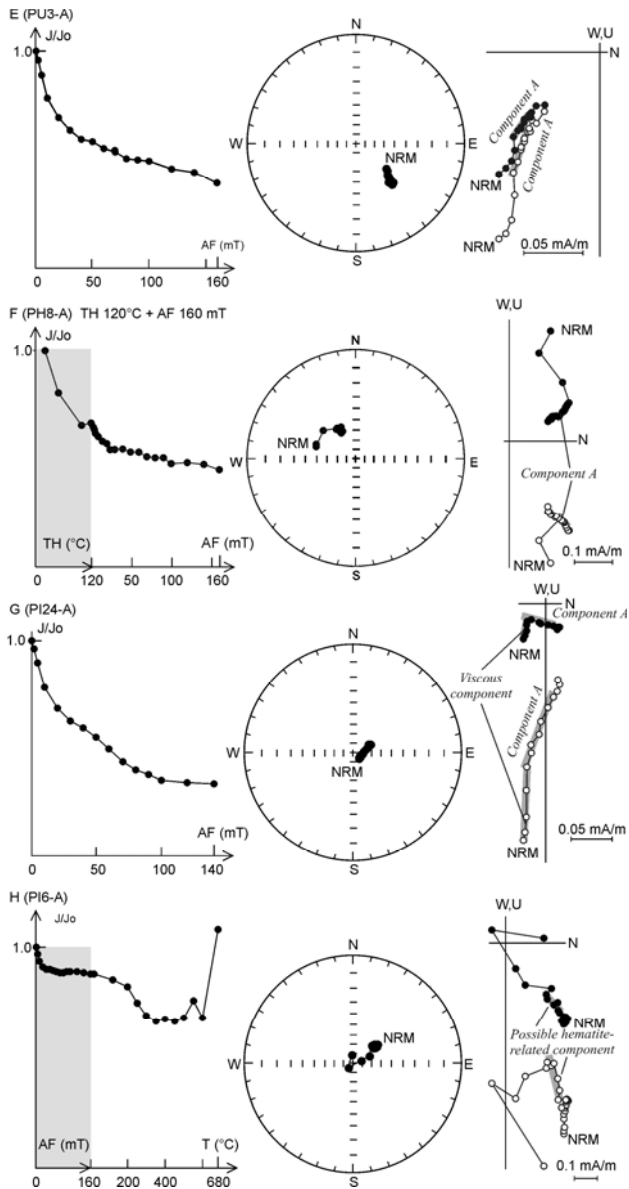


Fig. 5. Examples of demagnetization behaviour of studied lithologies (see Fig. 1 and Table 1 for locations of samples). The figures on the left show relative intensity decay curves ( $J/J_0$ ), where the demagnetizing alternating field [mT] and/or temperature [°C] are given on the horizontal axis. The figures in the centre show stereographic projections of directional data during demagnetization. The figures on the right show orthogonal demagnetization diagrams, where open (closed) symbols denote vertical (horizontal) planes. Data are in geographic coordinates.

Table 2

Component A remanence directions of individual sites before (subscript G) and after (subscript S) applying the bedding correction

| Location   | Site | $N/n$                | $D_G$<br>[°] | $I_G$<br>[°] | $k$   | $\alpha_{95}$<br>[°] | $D_S$<br>[°] | $I_S$<br>[°] |
|------------|------|----------------------|--------------|--------------|-------|----------------------|--------------|--------------|
| Tornimägi  | ►TM  | *5/5                 | 168.5        | 70.2         | 134.8 | 6.6                  | 173.9        | 66.8         |
| Pargimägi  | ►PM  | *2/24                | 70.8         | 76.4         | 33.4  | 44.7                 | 160.0        | 63.6         |
| Udria      | UD   | No stable components |              |              |       |                      |              |              |
| Laagna     | ►LG  | *7/10                | 138.4        | 65.1         | 25.7  | 12.1                 | 140.9        | 61.3         |
|            | LA   | *8/11                | 134.1        | 65.3         | 111.8 | 5.3                  | 133.9        | 60.3         |
| Meriküla   | ME   | No stable components |              |              |       |                      |              |              |
| Puhkova    | PH   | *8/8                 | 309.8        | 37.1         | 31.5  | 10.0                 | 309.0        | -25.6        |
|            | ►PK  | *5/9                 | 122.5        | 66.2         | 125.9 | 6.8                  | 142.0        | 55.6         |
|            | PU   | *10/10               | 344.8        | 64.1         | 50.0  | 6.9                  | 127.1        | 42.6         |
|            | PO   | No stable components |              |              |       |                      |              |              |
| Pähklimägi | ►PG  | *8/9                 | 126.6        | 77.8         | 33.3  | 9.7                  | 151.3        | 70.4         |
|            | PL   | No stable components |              |              |       |                      |              |              |
|            | PI   | *15/16               | 154.4        | 66.4         | 69.2  | 4.6                  | 131.7        | 75.8         |

was identified in the course of AF demagnetization (Fig. 5A), as the component carried by hematite was behaving unstable. The grey biomorphic limestones (Fig. 2A) of Pargimägi (PM) include big dolomite crystals within the fine-grained calcite matrix. Magnetite was identified by SEM studies (Fig. 2D), but very rare hematite or goethite occurs, too. Additionally to the viscous component, easily removed during the first steps of AF demagnetization, the samples include only component A, unblocking at 50-60 mT (Fig. 5B). Udria (UD) limestones have a strong viscous component in a direction of PEF due to goethite ooids (Fig. 2B, Fig. 3E); no other components were observed. In Laagna, two sites (LG and LA) were sampled and analysed. According to magnetic mineralogy studies, the partly dolomitized limestones (Fig. 2C) carry (Ti-)magnetite, hematite, and goethite (Figs. 3B, 4A and D). After heating up to 120°C, component A unblocks at ~60 mT in the course of AF demagnetization (Fig. 5C) and shows a coherent direction (Table 2) from sample to sample, but the remaining (after AF demagnetization up to 160 mT) high-coercivity remanence component directions are highly scattered. No stable components were identified in Meriküla (ME) dark grey dolomitized limestones, where the rock magnetic studies show the presence of high coercivity ferromagnetic minerals. According to TH demagnetization results, the component by goethite is towards the PEF (Fig. 5D). In Puhkova, four sites (PH, PK, PU, and PO) of Kunda stage dolomitized limestones

were analysed. Three of them (PH, PK, and PU) carry component *A* (see Table 2; Fig. 5F). The high coercivity component is unstable or points toward the PEF. In Pähklmägi, three sites (PG, PL, and PI) were sampled and analysed. According to the rock magnetic studies, these Kunda stage dolomitized limestones carry (Ti-)magnetite, hematite (Figs. 3D and 4B), and minor amount of goethite. The component *A* unblocks at <70 mT and shows a direction in PI and PG (Table 2; Fig. 5G) similar to A-type directions in other locations. A possible hematite-related NE-directed component (Fig. 5H) exists.

#### 4. DISCUSSION

Stability of component *A* was checked by the direction-correction (DC) tilt test (Enkin 2003). The test revealed optimal clustering at  $74.3 \pm 16.1\%$  un-tilting, thus, giving an indeterminate result (Fig. 6A). Assuming the deformation is of relatively recent glaciotectonic origin (Müdel *et al.* 1969, Rattas and Kalm 2004, Vaher *et al.* 2013), they post-date the observed primary magnetization (component *A*). There are two possible reasons for the ambiguous tilt test: imperfect separation of the component *A* and/or rotation of sedimentary blocks around their vertical axes. Excluding observations from four sites (PH, PI, PU, and LA; Fig. 1) gives, however, a positive tilt test result (optimal clustering at  $90.2 \pm 25.9$  unfolding; sites PK, PM, TM, PG, and LG; Figs. 1 and 6B). This choice of sites for mean calculations is also supported by inclination-only data: precision of mean inclination is higher in stratigraphic coordinates compared to that in geographic coordinates (in geographic coordinates:  $I_G = 71.9^\circ$ , precision parameter  $\kappa_G = 117.0$ , angular standard deviation  $\Theta_{63G} = 7.5^\circ$ , and 95 % confidence limit  $\alpha_{95G} = 7.1$ ; in stratigraphic coordinates:  $I_S = 64.0^\circ$ ,  $\kappa_S = 128.2$ ,  $\Theta_{63S} = 7.1^\circ$ ,  $\alpha_{95S} = 6.8$ ; see Arason and Levi 2010).

In order to define the age of component *A*, the corresponding palaeomagnetic pole (Table 3) was plotted on the Apparent Polar Wander Path (APWP) for Baltica (Fig. 7B) (Torsvik and Cocks 2005). The comparison confirms early Darriwilian age (466–467 Ma) for pole *A* [ $Lat = 17.9^\circ N$ ,  $Long = 47.3^\circ E$ ,  $K = 46.7$ ,  $A_{95} = 11.3^\circ$  (Table 3); calculations are based on data from 5 sites (Table 2) which pass positively the DC tilt test]. The pole coincides with the poles obtained from the approximately same stratigraphic sequences in Scandinavia and St. Petersburg area in Russia (Claesson 1978, Torsvik and Trench 1991a, Perroud *et al.* 1992, Torsvik *et al.* 1995, Smethurst *et al.* 1998, Khramov and Iosifidi 2009, Figs. 1A and 6B). Compared to our earlier observations (Plado *et al.* 2010, Dapingian and Darriwillan  $Lat = 11.4^\circ N$ ,  $Long = 39.1^\circ E$ ), a minor difference however exists. Based on the higher number of sites, shorter depositional time, and posi-

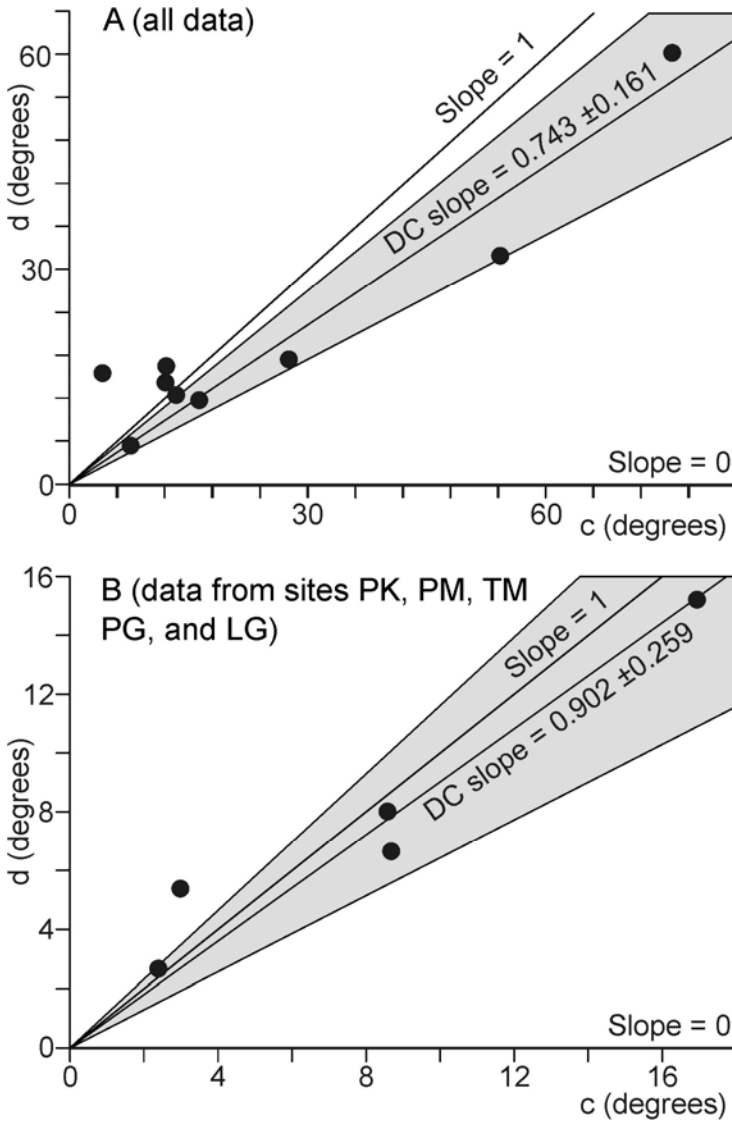


Fig. 6. Results of the DC tilt test (Enkin 2003) including data from (A) 9 sites and (B) 5 sites (see Table 2). (A) shows that the DC slope is different from either 1 or 0, resulting in an indeterminate tilt test. The DC slope in (B) is not significantly different from 1, but is significantly different from 0, indicating the remanence to be pre-folding in age and the carbonate layers from listed sites have not suffered significant rotation around their vertical axes.

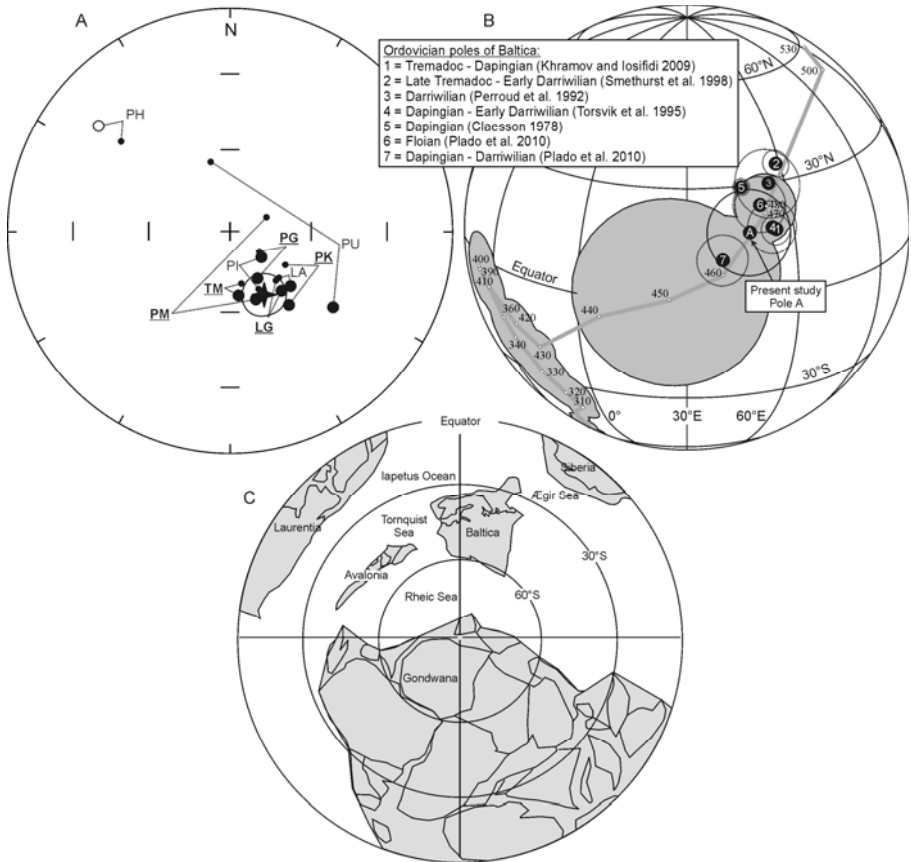


Fig. 7: (A) Equal-area stereonet projection of site means in geographic (small symbols) and stratigraphic (big symbols) coordinates. All the symbols denote downward pointing remanence. For site mean values, reference directions, and corresponding virtual geomagnetic pole positions, see Table 3. (B) Combination of Apparent Polar Wander Path (thick grey line) for Baltica (for 530–310 Ma) with running mean poles (Ma) and  $A_{95}$  confidence areas after Torsvik and Cocks (2005). Pole of the present study (A; Table 3) is shown with black circle. The black numbered circles and squares represent palaeomagnetic poles from preceding studies (see text and insert for details). (C) Plate reconstruction for 470–460 Ma. Baltica is positioned according to the present (pole A) data. Other continents are positioned after APWP suggested by Torsvik *et al.* (2012).

tive tilt test, we assume the present pole is more reliable. Lack of dual polarity in our A-poles suggests that our data belong to the long-lasting reversed “Moyero” polarity epoch (*e.g.*, Pavlov and Gallet 2005; see also



Torsvik and Trench 1991b, Torsvik *et al.* 1995) prevailing in the Early and Middle Ordovician.

Table 3

Mean remanence direction of component A as transferred to the reference city (after bedding correction) and corresponding virtual geomagnetic pole

| Comp     | Polarity | $B/N/n$  | $D_{\text{ref}} \pm D_{\text{ref}}$<br>[°] | $I_{\text{ref}} \pm I_{\text{ref}}$<br>[°] | Plat | Plon | $K$  | $A_{95}$ |
|----------|----------|----------|--|--|------|------|------|----------|
| <i>A</i> | <i>R</i> | *5/43/68 | 154.6 ± 15.3                               | 60.9 ± 9.7                                 | 17.9 | 47.3 | 46.7 | 11.3     |

**Notice:** Comp. = characteristic remanence component,  $B/N/n$  = number of sites/samples/specimens revealing A (passing positively the direction-correction (DC) tilt test of Enkin (2003) has been taken into consideration; the level of statistics is indicated by asterisks),  $D_{\text{ref}}$  and  $I_{\text{ref}}$  = reference declination and inclination of the mean magnetization with confidence limits ( $\Delta D_{\text{ref}}$  and  $\Delta I_{\text{ref}}$ ) calculated with respect to the reference city (Kajaani, Finland; 64.1°N, 27.7°E), Plat and Plon = the latitude and longitude of the pole;  $K$  = Fisher's (1953) precision parameter;  $A_{95}$  = the radius of a cone of 95% confidence about the mean pole.

Based on present results, component *A* is most likely carried by PSD and/or SD magnetite. The tilt test and similarity of the pole with those obtained by other regional studies (summarized by Torsvik *et al.* 2012) hint that the magnetization was acquired before tilting and likely during or soon after sedimentation. Magnetite in marine carbonates, including limestones formed in the open shelf conditions, is likely detrital in origin (Kirschvink and Chang 1984), and acquisition of a stable primary natural remanence is linked to sediment-water interface (DRM), postdepositional alignment processes (pDRM; *e.g.*, Lowrie and Heller 1982, Elmore *et al.* 1994, Karlin *et al.* 1987), and/or activity of magnetotactic bacteria (Mao *et al.* 2014). If the detrital origin is real, release of iron into the ocean has been fast enough not affording the  $\text{Fe}^{2+}$ -bearing minerals being oxidized when brought into contact with oxygen and not involved in transport (see, *e.g.*, Raiswell 2011).

The present result (pole *A*) places Baltica at mid-southerly latitudes (Fig. 7C) with the present Caledonian longitudinal axis oriented almost east-west. The position agrees with latest (see Torsvik *et al.* 2012) Ordovician palaeogeographic reconstruction of Baltica describing that during the Middle and Late Ordovician, Baltica, being located at southern hemisphere, drifted northwards and suffered significant ( $\sim 2^\circ/\text{Ma}$ ) anti-clockwise rotation (see also Smethurst *et al.* 1998, Torsvik and Cocks 2005). Latitudinal velocity of the northward drift reached almost 10 cm/yr in the Late Ordovician and Early Silurian (Torsvik *et al.* 2012) until destruction of Iapetus Ocean and the Caledonian collision between Baltica and Laurentia starting in mid-Silurian.

## 5. CONCLUSIONS

A characteristic remanent magnetization component was identified in the early Darriwilian (Kunda and Aseri regional stages) glaciotectonically tilted carbonate sequence of NE Estonia. This south-easterly downwards directed remanence component A (found in 9 sites out of 13) dates to the Middle Ordovician (~465 Ma). The glaciotectonic event has, however, caused some rotation of sampled blocks as the DC tilt test (Enkin 2003) results were ambiguous. Nevertheless, directional data of component A from 5 selected sites (Figure 1, Table 2) passed the tilt test positively suggesting that the rotational movements were not comprehensive. Remanence data from these five sites gave virtual geomagnetic south pole at latitude 17.9°N and longitude 47.3°E ( $K = 46.7$ ,  $A_{95} = 11.3$ ), which fits with Middle Ordovician APWP of Baltica Plate. Component A has reversed polarity matching a long-lasting reversed “Moyero” polarity epoch prevailing in the Early and Middle Ordovician (Pavlov and Gallet 2005). As revealed by mineralogical studies, the component A is resident in magnetite, whose origin is detrital or post-depositional produced during early diagenesis.

**Acknowledgment** We acknowledge comments into the earlier version of the manuscript made by A. Biggin, C. Mac Niocaill, M. Mattei, and E.L. Pueyo. The Estonian Science Foundation (grants # 7860 and 8701) and Estonian Ministry of Education and Research (grants IUT20-34 and SF0180069s08) supported the study. We thank J. Grabowski and an anonymous reviewer for their comments and improvements.

## References

- Arason, P., and S. Levi (2010), Maximum likelihood solution for inclination-only data in paleomagnetism, *Geophys. J. Int.* **182**, 2, 753-771, DOI: 10.1111/j.1365-246X.2010.04671.x.
- Claesson, C. (1978), Swedish Ordovician limestones: Problems in clarifying their directions of magnetizations, *Phys. Earth Planet. Int.* **16**, 1, 65-72, DOI: 10.1016/0031-9201(78)90101-2.
- Elmore, R.D., K. Cates, G. Gao, and L. Land (1994), Geochemical constraints on the origin of secondary magnetizations in the Cambro-Ordovician Royer Dolomite, Arbuckle Mountains, southern Oklahoma, *Phys. Earth Planet. Int.* **85**, 1-2, 3-13, DOI: 10.1016/0031-9201(94)90004-3.
- Enkin, R.J. (2003), The direction-correction tilt test: an all-purpose tilt/fold test for paleomagnetic studies, *Earth Planet. Sci. Lett.* **212**, 1-2, 151-166, DOI: 10.1016/S0012-821X(03)00238-3.

- Fisher, R. (1953), Dispersion on a sphere, *Proc. Roy. Soc. London A* **217**, 1130, 293-305, DOI: 10.1098/rspa.1953.0064.
- Hirt, A.M., A. Banin, and A.U. Gehring (1993), Thermal generation of ferromagnetic minerals from iron-enriched smectites, *Geophys. J. Int.* **115**, 3, 1161-1168, DOI: 10.1111/j.1365-246X.1993.tb01518.x.
- Jaansoon-Orviku, K. (1926), Rändpangaseid Eestis, *LUS Aruanded* **33**, 48-56 (in Estonian).
- Karlin, R., M. Lyle, and G.R. Heath (1987), Authigenic magnetite formation in suboxic marine sediments, *Nature* **326**, 6112, 490-493, DOI: 10.1038/326490a0.
- Khramov, A.N., and A.G. Iosifidi (2009), Paleomagnetism of the Lower Ordovician and Cambrian sedimentary rocks in the section of the Narva river right bank: For the construction of the Baltic kinematic model in the Early Paleozoic, *Izv., Phys. Solid Earth* **45**, 6, 465-481, DOI: 10.1134/S1069351309060019.
- Kirschvink, J.L. (1980), The least-squares line and plane and the analysis of palaeomagnetic data, *Geophys. J. Roy. Astr. Soc.* **62**, 3, 699-718, DOI: 10.1111/j.1365-246X.1980.tb02601.x.
- Kirschvink, J.L., and S.-B.R. Chang (1984), Ultra fine-grained magnetite in deep-sea sediments: possible bacterial magnetofossils, *Geology* **12**, 9, 559-562, DOI: 10.1130/0091-7613(1984)12<559:UMIDSP>.
- Lowrie, W. (1990), Identification of ferromagnetic minerals in a rock by coercivity and unblocking temperature properties, *Geophys. Res. Lett.* **17**, 2, 159-162, DOI: 10.1029/GL017i002p00159.
- Lowrie, W., and F. Heller (1982), Magnetic properties of marine limestones, *Rev. Geophys. Space Phys.* **20**, 2, 171-192, DOI: 10.1029/RG020i002p00171.
- Mao, X., R. Egli, N. Petersen, M. Hanzlik, and X. Zhao (2014), Magnetotaxis and acquisition of detrital remanent magnetization by magnetotactic bacteria in natural sediment: First experimental results and theory, *Geochem. Geophys. Geosyst.* **15**, 1, 255-283, DOI: 10.1002/2013GC005034.
- Miidel, A., Ü Paap, A. Raukas, and E. Rähni (1969), On the origin of the Vaivara Hills (Sinimäed) in NE Estonia, *Proc. Estonian Ac. Sci. Chem. Geol.* **18**, 370-376.
- Özdemir, Ö., and D.J. Dunlop (1996), Thermoremanence and Néel temperature of goethite, *Geophys. Res. Lett.* **23**, 9, 921-924, DOI: 10.1029/96GL00904.
- Pavlov, V., and Y. Gallet (2005), A third superchron during the Early Paleozoic, *Episodes* **28**, 2, 1-6.
- Perroud, H., M. Robardet, and D.L. Bruton (1992), Palaeomagnetic constraints upon the palaeogeographic position of the Baltic Shield in Ordovician, *Tectonophysics* **201**, 1-2, 97-120, DOI: 10.1016/0040-1951(92)90178-9.
- Plado, J., U. Preeden, L.J. Pesonen, S. Mertanen, and V. Puura (2010), Magnetic history of Early and Middle Ordovician sedimentary sequence, northern Esto-

- nia, *Geophys. J. Int.* **180**, 1, 147-157, DOI: 10.1111/j.1365-246X.2009.04406.x.
- Puura, V., and R. Vaher (1997), Cover structure. **In:** A. Raukas and A. Teedumäe (eds.), *Geology and Mineral Resources of Estonia*, Estonian Academy Publishers, Tallinn, 167-177.
- Raiswell, R. (2011), Iron transport from the continents to the open ocean: The aging-rejuvenation cycle, *Elements* **7**, 2, 101-106, DOI: 10.2113/gselements.7.2.101.
- Rattas, M., and V. Kalm (2004), Glaciotectonic deformation patterns in Estonia, *Geol. Q.* **48**, 1, 15-22.
- Roberts, A.P., Y. Cui, and K.L. Verosub (1995), Wasp-waisted hysteresis loops: Mineral magnetic characteristics and discrimination of components in mixed magnetic systems, *J. Geophys. Res.* **100**, B9, 17909-17924, DOI: 10.1029/95JB00672.
- Shive, P.N., and J.F. Diehl (1997), Reduction of hematite to magnetite under natural and laboratory conditions, *Adv. Earth Planet. Sci.* **1**, 113-122, DOI: 10.1007/978-94-010-1286-7\_8.
- Smethurst, M.A., A.N. Khramov, and S. Pisarevsky (1998), Palaeomagnetism of the Lower Ordovician Orthoceras Limestone, St. Petersburg, and a revised drift history for Baltica in the early Palaeozoic, *Geophys. J. Int.* **133**, 1, 44-56, DOI: 10.1046/j.1365-246X.1998.1331463.x.
- Suuroja, K., T. Mardim, K. Ploom, T. All, M. Otsmaa, and M. Kõiv (2009), *The Explanatory Note to the Geological Maps of Narva*, 6534 sheet. Tallinn, Geological Survey of Estonia, 127 pp.
- Tarling, D.H. (1983), *Paleomagnetism*, Chapman and Hall, London, 397 pp.
- Torsvik, T.H., and L.R.M. Cocks (2005), Norway in space and time: A Centennial cavalcade, *Norwegian J. Geol.* **85**, 1-2, 73-86.
- Torsvik, T.H., and E.F. Rehnström (2003), The Tornquist Sea and Baltica-Avalonia docking, *Tectonophysics* **362**, 1-4, 67-82, DOI: 10.1016/S0040-1951(02)00631-5.
- Torsvik, T.H., and M.A. Smethurst (1999), Plate tectonic modelling: virtual reality with GMAP, *Comput. Geosci.* **25**, 4, 395-402, DOI: 10.1016/S0098-3004(98)00143-5.
- Torsvik, T. H., and A. Trench (1991a), The Lower-Middle Ordovician of Scandinavia: Southern Sweden “revisited”, *Phys. Earth Planet. Int.* **65**, 3-5, 283-291, DOI: 10.1016/0031-9201(91)90135-5.
- Torsvik, T.H., and A. Trench (1991b), Ordovician magnetostratigraphy: Llanvirn-Caradoc limestones of the Baltic platform, *Geophys. J. Int.* **107**, 1, 171-184, DOI: 10.1111/j.1365-246X.1991.tb01165.x.
- Torsvik, T.H., A. Trench, K.C. Lohmann, and S. Dunn (1995), Lower Ordovician reversal asymmetry – an artifact of remagnetization or nondipole field disturbance, *J. Geophys. Res.* **100**, B9, 17885-17898, DOI: 10.1029/95JB00667.

- Torsvik, T.H., R. Van der Voo, U. Preeden, C. Mac Niogaill, B. Steinberger, P.V. Doubrovine, D.J.J. van Hinsbergen, M. Domeier, C. Gaina, E. Tohver, J.G. Meert, P.J.A. McCausl, and L.R.M. Cocks (2012), Phanerozoic polar wander, palaeogeography and dynamics, *Earth Sci. Rev.* **114**, 3-4, 325-368, DOI: 10.1016/j.earscirev.2012.06.007.
- Vaher, R., A. Miidel, and A. Raukas (2013), Structure and origin of the Vaivara Sinimäed hill range, Northeast Estonia, *Estonian J. Earth Sci.* **62**, 3, 160-170, DOI: 10.3176/earth.2013.13.
- Walker, J.D., J.W. Geissman, S.A. Bowring, and L.E. Babcock (2012), Geologic time scale, ver. 4.0, Geological Society of America, DOI: 10.1130/2012.CTS004R3C.
- Zijderveld, D.J. (1967), A.C. demagnetization in rocks: analysis of results. **In:** W.D.W. Collinson *et al.* (eds.), *Methods in Paleomagnetism*, Elsevier, Amsterdam, 254-286.

Received 16 March 2015

Received in revised form 5 November 2015

Accepted 21 December 2015